

Hole localization in Al doped silica: A DFT+U description

Michael Nolan and Graeme W. Watson

Citation: *J. Chem. Phys.* **125**, 144701 (2006); doi: 10.1063/1.2354468

View online: <http://dx.doi.org/10.1063/1.2354468>

View Table of Contents: <http://jcp.aip.org/resource/1/JCPSA6/v125/i14>

Published by the American Institute of Physics.

Additional information on J. Chem. Phys.

Journal Homepage: <http://jcp.aip.org/>

Journal Information: http://jcp.aip.org/about/about_the_journal

Top downloads: http://jcp.aip.org/features/most_downloaded

Information for Authors: <http://jcp.aip.org/authors>

ADVERTISEMENT

physicstoday

Comment on any
Physics Today article.

Physics Today / Volume 65 / Issue 7 / July 2012
Previous Article | Next Article

Measured energy in Japan
David von Seggern
(vonseg@seismo.unr.edu) University of Nevada
July 2012, page 10
DIGITAL OBJECT IDENTIFIER
<http://dx.doi.org/10.1063/PT.3.1619>

The article by Thorne Lay and Hiroo Kanamori is an interesting one. It discusses the energy released by the 2011 Tohoku earthquake. The authors estimate that the earthquake released approximately five times as much energy as the 1909 San Francisco earthquake. This is a significant finding, as it suggests that the energy released by earthquakes is much larger than previously estimated. The authors also discuss the implications of this finding for the design of nuclear reactors. They argue that the energy released by earthquakes is a significant source of seismic energy, and that this energy can be used to power nuclear reactors. This is a novel idea, and it is one that deserves further investigation.

By the act of hitting a ball with a bat, one calculates the force energy to deliver the ball to its new location, but one must also take into account that the ball extended its energy release to that which became struck by the ball as its momentum ceased and passed energy to the struck team. Therefore the parameters of the damage extend into the future when the received energy to that pushed upon later becomes released in a new event. Perhaps calculations of one added that in while another's calculations did not. E.M.C.
Written by Edgar McCarvill, 14 July 2012 19:59

Hole localization in Al doped silica: A DFT+*U* description

Michael Nolan^{a)} and Graeme W. Watson^{b)}

School of Chemistry, University of Dublin, Trinity College, Dublin 2, Ireland

(Received 26 May 2006; accepted 18 August 2006; published online 10 October 2006)

Despite density functional theory (DFT) being the most widely used *ab initio* approach for studying the properties of oxide materials, the modeling of localized hole states in doped or defective oxides can be a challenge. The electronic hole formed when silica is doped with aluminum is such a defect, for which a DFT description of the atomic and electronic structures has previously been found to be inconsistent with experiment, while Hartree-Fock provides a consistent description. We have applied the DFT+*U* approach to this problem and find that the structural distortions around the dopant are consistent with experimental data as well as earlier cluster calculations using Hartree-Fock and perturbation theory. A hole state is found 1.1 eV (1.6 eV experimentally) above the top of the valence band with localization of spin on the oxygen atom which shows the elongated Al–O distance. A formation energy of 5.7 eV is found. We discuss implications for using DFT+*U* to model defective oxide systems with O 2*p* holes. © 2006 American Institute of Physics. [DOI: 10.1063/1.2354468]

I. INTRODUCTION

Although periodic plane wave density functional theory (DFT) is a standard approach for the study of oxide materials, there are a number of systems where it fails to provide even a qualitatively correct description of the geometry and electronic structure. These systems include some transition and rare earth metal oxides as well as rare earth metals and are characterized by the presence of highly localized *d* and *f* metal states; well known examples of this problem are NiO and FeO (with *d* states) (Refs. 1 and 2) and reduced CeO₂ (Refs. 3 and 4) and Ce metal (with *f* states).⁵

In recent years the strongly localized O 2*p* derived hole states found in metal oxides upon substitutional doping of the cation with a metal ion which has one less electron have been incorrectly described with standard plane wave periodic DFT. Interesting examples of this phenomenon include Li doped MgO (Refs. 6 and 7) and Al doped silica (SiO₂).^{8–10} In both cases, electron paramagnetic resonance spectroscopy (EPR) shows the presence of a single unpaired electron localized on one oxygen atom.^{6,8} It has also been demonstrated that a structural distortion is present which is manifested as a single elongated dopant-oxygen distance. The electronic hole resides on the oxygen atom with the elongated dopant-oxygen distance.

The application of DFT to Al-doped SiO₂ yields an electronic hole delocalized over the four oxygen atoms coordinated to the dopant, with no structural distortions, both of which contradict the experiment.^{9,10} Given the success of DFT in describing oxide properties, it was speculated that the experimental interpretation was incorrect.¹¹ However, since plane wave approaches cannot compute hyperfine coupling

constants for comparison with EPR data, it was not possible to conclude whether DFT is incorrect or experimental data were incorrectly interpreted.

Cluster models have been applied to this problem.^{10–12} While issues associated with the finite size of a cluster are present, the results bear out that for this system a cluster model description is adequate.^{10–12} With an all-electron basis set, cluster models allow the calculation of hyperfine coupling parameters for comparison with experiment. Applying spin unrestricted Hartree-Fock (UHF) to this problem results in a distorted geometry with one elongated Al–O distance and localization of the electronic hole on the oxygen atom in the elongated Al–O bond.^{10–12} A description of this system with pure DFT functionals gives the same result as the earlier plane wave calculations, while hybrid DFT (using B3-LYP) with 20% HF exchange results in a structure where the electronic hole is spread over two O atoms.¹¹ Pacchioni *et al.* showed that the combination of UHF exchange and LYP correlation provided a similar description of the atomic and electronic structures as UHF,¹¹ while To *et al.* used the BB1K hybrid functional, with 42% exact exchange, to obtain atomic and electronic structures consistent with experiment.¹² Finally, calculation of the hyperfine coupling constants with UHF, UHF-LYP, and BB1K yielded results that are in reasonable agreement with experiment, while with pure DFT functionals and B3-LYP the agreement with experiment was poor.^{10–12} These results help establish the original interpretation of the EPR spectra for Al doped SiO₂ and demonstrate that the problem with DFT is rooted in the description of exchange. Cluster models suffer from a number of deficiencies related to basis set choice and size of the quantum part of the cluster, both of which require some investigation.

The failure of DFT to describe, even qualitatively, the atomic and electronic structures of Al doped SiO₂ (Refs. 8 and 9) indicates its limited applicability to the study of de-

^{a)}Present address: Tyndall National Institute, Lee Maltings, Prospect Row, Cork, Ireland. Electronic mail: michael.nolan@tyndall.ie

^{b)}FAX: +353 1627 2862. Electronic mail: watsong@tcd.ie

fective systems. While the above discussion illuminates the effect of having a proper description of exact exchange in order to obtain a consistent description of Al doped SiO_2 , the calculations involve cluster models. It would be useful to have an approach that can provide a consistent description, but in a periodic plane wave basis. Current exchange-correlation functionals use an approximation for the exchange contribution which does not cancel with the Hartree interaction for a single electron, and thus a single electron interacts with its own charge density. This self-interaction error (SIE) introduces an energy penalty for localization of a single electron and causes incorrect delocalization when using pure DFT. The DFT+ U approach¹³ adds an orbital dependent term, much like HF exchange, which accounts for the on-site electron-electron interaction and correctly localizes the electron. The parameter U controls the strength of this interaction and is determined for defective and doped systems through a comparison with the available experimental data, whereupon the best choice of U is made. Traditionally, this approach is applied to systems where the partially occupied d and f states are inconsistently described with DFT. In ongoing work in the study of defective oxides, we have successfully applied the DFT+ U approach to Li doped MgO ,⁷ demonstrating that this approach, which was originally applied to cation d and f states in oxides, can also be applied to localized O $2p$ hole states. In that work, the value of U that was determined from comparison with experiment was 7 eV.

In this paper, we focus on applying the DFT+ U methodology to the problem of Al doped silica. We will discuss the inability of generalized gradient approximation (GGA)-DFT to describe Al doped silica, even qualitatively, and demonstrate the effect of U on the atomic and electronic structures around the dopant. From this, we obtain a suitable value of U and discuss the atomic and electronic structures of Al doped silica. We also present a discussion of the general applicability of the DFT+ U approach to these materials.

II. METHODS

We apply plane wave based density functional theory, as implemented in the Vienna *ab initio* simulation package (VASP).^{14,15} The electronic states of the valence electrons are expanded in a basis of plane waves, the cutoff of which is set to 500 eV. To describe the core-valence interaction, we use Blöchl's projector augmented wave approach^{16,17} (PAW), which is in essence an all-electron calculation with a frozen core; the cores are Si and Al [Ne] and O [He]. The Perdew-Burke-Ernzerhof exchange correlation functional¹⁸ (PBE) is used, with the electronic states sampled using a $2 \times 2 \times 2$ Monkhorst-Pack k -point sampling mesh.

A simulation cell containing 24 oxygen, 11 silicon, and 1 Al atom is used throughout the calculations with unit cell parameters, $a=b=9.826$ Å and $c=5.405$ Å. All ions are fully relaxed using a quasi-Newton scheme until the forces are less than 0.01 eV/Å. For the DFT+ U calculations, we use Dudarev's approach,¹³ as implemented in VASP. Similar to previous studies, we vary the value of U from 0 (GGA) to

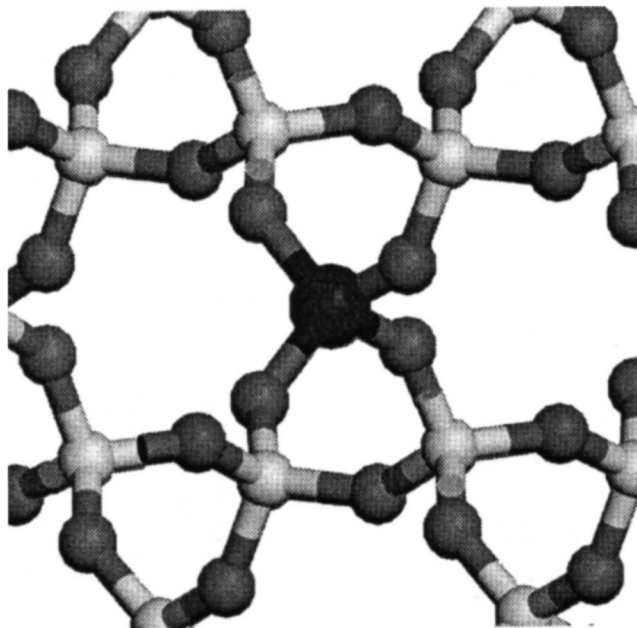


FIG. 1. Geometry around the Al dopant in silica. The dopant, Al, is the large black sphere, the silicon atoms are the light colored spheres, and the oxygen atoms are the dark gray spheres.

7 eV and choose that value of U that provides an electronic structure consistent with experiment.

III. RESULTS

A. GGA-DFT description of doped silica

A full ionic relaxation of doped silica (Fig. 1) was carried out with GGA. Two starting structures were considered throughout. The first is symmetric, with two pairs of Al–O distances, while in the second we distort one of the Al–O distances to break this symmetry. This is necessary, since the distorted and undistorted structures can be local minima.^{10,11} In both cases, the GGA calculation results in the same final structure with two pairs of Al–O distances, 1.75 and 1.73 Å, while the nearest Si–O distances are 1.59 Å, in good agreement with other periodic DFT calculations.^{10,11}

The O $2p$ ion and angular momentum decomposed partial electronic density of states (PEDOS) are shown in Fig. 2 for spin up and spin down electrons. We see that between the

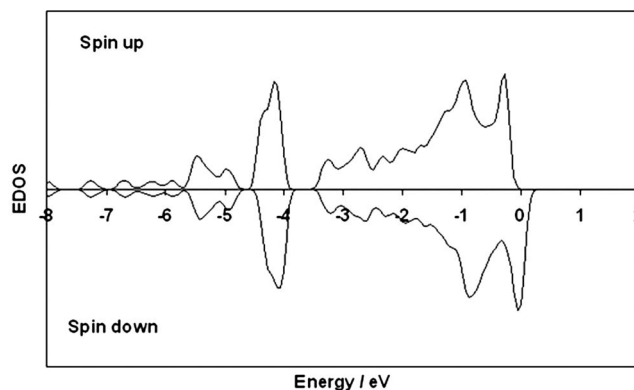


FIG. 2. GGA O $2p$ PEDOS for Al doped silica for the four oxygen atoms surrounding the Al dopant.

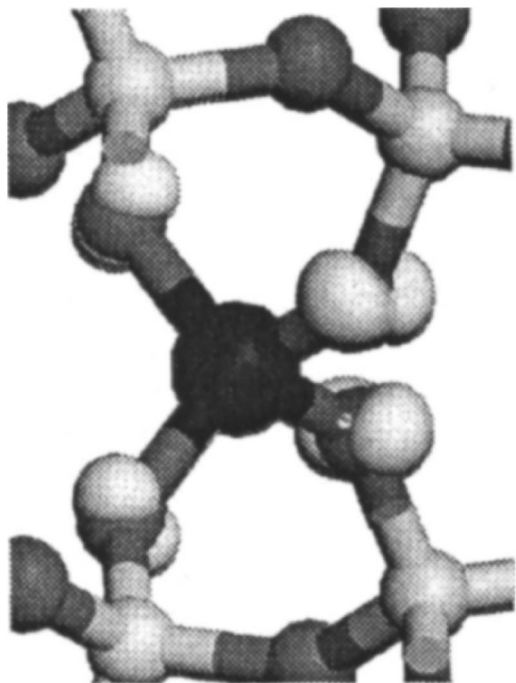


FIG. 3. GGA spin density for Al doped silica. The isosurface contours are $0.11 e/\text{\AA}^3$.

top of the valence band (the energy zero) and the conduction band no gap state is present. The spin density (defined as the difference between the up spin and the down spin densities) is plotted in Fig. 3. This shows clearly delocalization of excess spin over the four oxygen atoms around the Al dopant. Thus, the GGA description of Al doped SiO_2 is inconsistent with experiment and calculations which include exact exchange.^{10,11}

B. DFT+*U* description of doped silica

To address the problem with GGA-DFT discussed above, we recognize that the incorrect description of Al doped SiO_2 is caused by the self-interaction error present in approximate DFT exchange-correlation functionals. One approach has been to mix into the calculation a degree of exact exchange as in hybrid DFT approaches.^{11,12} The degree of exact exchange is critical and could be considered as an empirical parameter, with too little resulting in delocalization (e.g., B3-LYP has 20% exact exchange) while BB1K, with 42% exchange, contains enough of a contribution to localize the charge density.¹² To overcome this difficulty with GGA-DFT and allow for calculations in a periodic plane wave basis, we make use of the DFT+*U* approach;¹³ we apply the *U* term to the O *2p* states and leave the Si and Al states to be described by GGA. We have tested values of *U* in the range of 1–7 eV, starting from the symmetric and slightly distorted structures discussed above, making comparison to available experimental data. While the symmetric structure, with two pairs of Al–O distances, is a local minimum in the potential energy surface for all values of *U*, the nature of the lowest energy structure depends on the value of *U* [similar to the dependence on the amount of exact exchange in hybrid DFT (Refs. 11 and 12)].

TABLE I. Al–O distances in Al doped silica as a function of *U*. For the GGA calculation, *U*=0 eV.

<i>U</i> eV	Al–O distances (Å)
GGA	$2 \times 1.75, 2 \times 1.73$
2	$2 \times 1.75, 2 \times 1.73$
3	$2 \times 1.75, 2 \times 1.72$
4	$2 \times 1.76, 2 \times 1.71$
5	$2 \times 1.76, 2 \times 1.71$
6	1.85, 1.72, 2×1.69
7	1.88, 1.71, 2×1.69

In Table I we present the Al–O distances as a function of *U* (the GGA calculations are equivalent to *U*=0 eV). Values of *U* up to 3 eV give a geometry that is little changed from the GGA result, i.e., a symmetric set of Al–O bonds with no distortion. For *U* between 3 and 6 eV, we find some Al–O elongation; however, it is a pair of Al–O bonds that elongate, rather than the single Al–O bond observed experimentally, consistent with the results of hybrid DFT with a small exchange contribution. For *U* greater than 6 eV, we find a description of the geometry that is consistent with the experimental data. In this geometry, we have one pair of Al–O distances around the dopant atom, which are 1.69 Å. There is a third Al–O distance at 1.71 Å and the final Al–O distance is substantially elongated at 1.88 Å (*U*=7 eV). This elongation is in good agreement with experimental observations⁸ and that found using HF, MP2, and BB1K hybrid DFT with a substantial exact exchange contribution.^{10–12}

To establish the effect of the dopant on the electronic structure, we examine the oxygen PEDOS. In Fig. 4 we display the total O *2p* EDOS for the four oxygen atoms surrounding the dopant for different values of *U*. The EDOS from the DFT+*U* calculation shows the effect of *U* on the electronic structure. For small values of *U*, we find a similar electronic structure to that obtained in the GGA calculation.

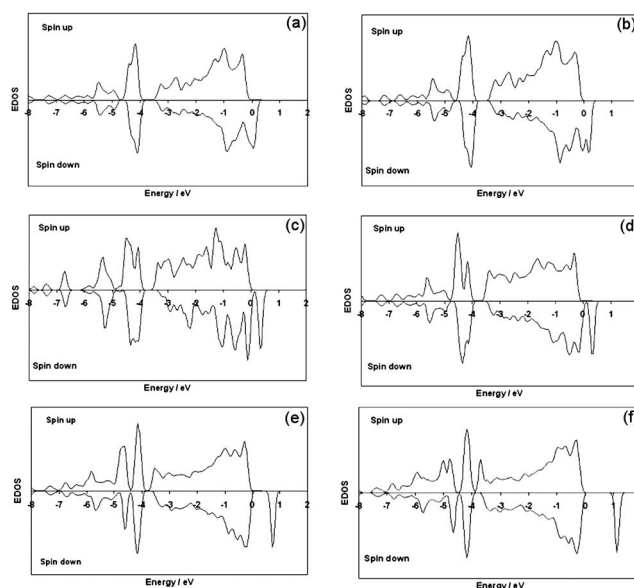


FIG. 4. O *2p* EDOS for Al doped SiO_2 for different values of *U*. The oxygen atoms considered are the four atoms surrounding the Al dopant. (a) 2 eV, (b) 3 eV, (c) 4 eV, (d) 5 eV, (e) 6 eV, and (f) 7 eV.

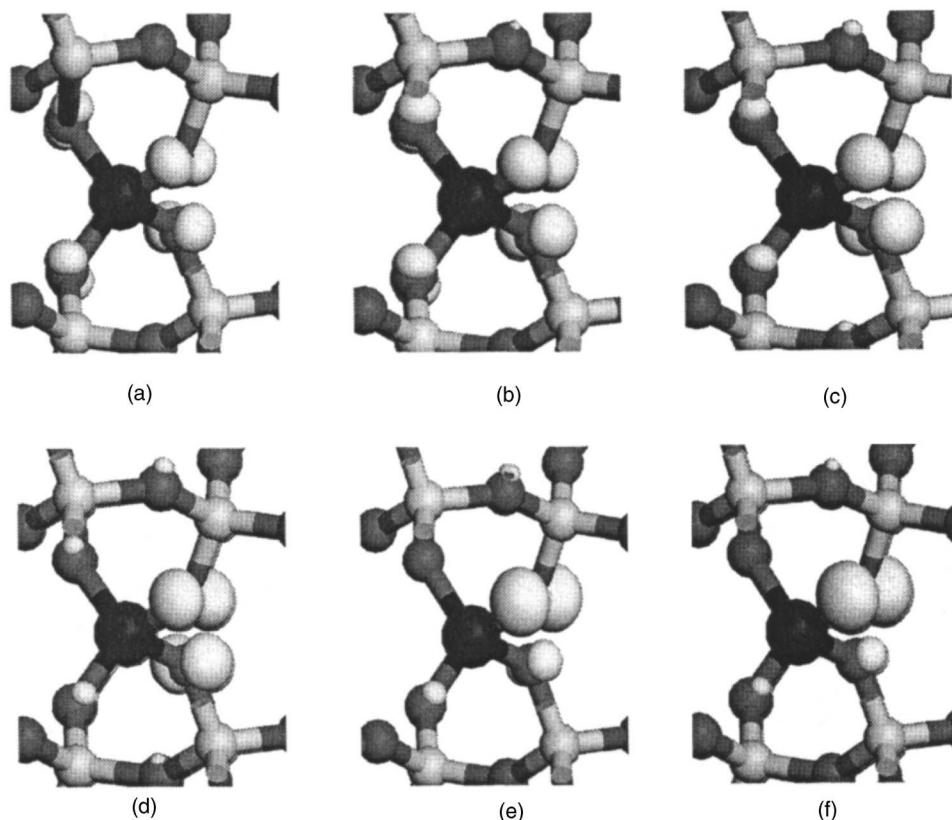


FIG. 5. Excess spin density for Al doped silica as a function of U . (a) 2 eV, (b) 3 eV, (c) 4 eV, (d) 5 eV, (e) 6 eV, and (f) 7 eV. The isosurface contours are $0.11 e/\text{\AA}^3$.

For $U=4/5$ eV, a new peak state appears; however, it is still very close to the valence band and the geometry shows that for this magnitude of U , there are still two pairs of Al–O distances. For U greater than 6 eV, a unoccupied state is obtained, which is well separated from the valence band, in agreement with experiment, while for these values of U , the geometry shows a single elongated Al–O distance. For $U=7$ eV, the offset from the top of the valence band to the gap states is 1.1 eV, compared to 1.6 eV determined experimentally.

To confirm the presence of a localized defect state on one oxygen atom neighboring the dopant, we present in Fig. 5 the spin density, defined as the difference in the up spin and down spin densities as a function of U . For the GGA calculation and for small values of U , the electronic hole introduced by doping with Al is delocalized over the four oxygen atoms neighboring the dopant, which is consistent with the geometric data presented in Table I. This is similar to the behavior observed with GGA-DFT when MgO is doped with lithium.⁷ For $U=4$ and 5 eV, the spin density is localized on two oxygen atoms surrounding the dopant, similar to that observed with B3-LYP.¹⁰

With $U=6$ or 7 eV, we find that localization of spin is present on a single oxygen atom. This is the oxygen atom with the distorted Al–O distance. With a plane wave basis set and core potentials such as PAW, it is not possible to compute hyperfine coupling constants, since these require an all-electron basis set that describes the electron density at the nucleus. However, there are a number of other results from this work that can be compared to previous experimental and computational studies.

The first point of agreement is in the local geometry

around the dopant site. With a correct choice of U , the present finding of elongation of one Al–O distance and the hole localization are consistent with cluster calculations as well as the available experimental data. While HF and HF coupled with a correlation functional as well as hybrid DFT (with a large proportion of exchange^{11,12}) are able to describe the structure of the defect and the hole localization, the present results are the first plane wave DFT with an appropriate approach (i.e., DFT+ U) to provide a consistent description of this defect. The energy required to form the Al-doped structure is 5.7 eV, and shows little dependence on the choice of U , while with GGA it is 5.68 eV. We note that the GGA formation energy is very close to that computed with DFT+ U . For CeO₂ and Li doped MgO, we have found small differences of 0.40 and 0.20 eV between DFT and DFT+ U for oxygen vacancy formation energies and Li doping energies, respectively. This suggests that in these cases, there must be some cancellation of error in the DFT calculation for the DFT defect formation energy to be so similar to the DFT+ U formation energy.

The present results demonstrate that the DFT+ U approach recovers a description of the geometrical and electronic structures of Al doped silica that is consistent with experimental data and calculations in which exact exchange is present, such as UHF.^{10,11} In a similar fashion, we found for Li doped MgO that the same value of U provided a consistent description of the atomic and electronic structures.⁷

In both cases, we have determined a value of U using experimental data. This raises an interesting question regarding the predictive ability of the DFT+ U method used in this work, in which the value of U is required to be determined

empirically through fitting to experimental data. Thus we have the question of what if experimental data were not available to which the value of *U* can be fitted? In addition, different ways of determining *U* or the form of the localized orbitals can impact on the results of a DFT+*U* calculation.

Fitting of *U* to experimental data has arisen in a number of published works where calculations seek to reproduce experimental observations. Amongst others, we mention the work of ourselves and Fabris on defective CeO₂,^{3,4} the early DFT+*U* calculations on NiO,^{1,19} and recent work from Gadjos and Hafner using DFT+*U* for CO adsorption on Pt(111), where the band gap of CO was used to fit a value of *U* to provide agreement with the experimentally characterized adsorption site.²⁰

Other DFT+*U* implementations can be found in the literature, e.g., the work of Cococcioni and de Gironcoli²¹ which has been applied to defective ceria.⁴ The interesting aspect of this DFT+*U* approach is that it uses localized Wannier orbitals and a linear response methodology to determine the value of *U* from first principles. In principle, there is no need to fit to experimental data so that this approach might be useful for predictive purposes, where experimental data are not available. However, the energetics do depend on the value of *U* and in published work, the authors do make use of experimental findings.⁴ Thus, a DFT+*U* approach still needs to be tested against the experiment.

While making use of particular experimental data is still a feature of DFT+*U* implementations, we note that the general feature of the present study—the description of O 2*p* electronic holes in oxides—has been investigated in many papers^{22–26} and we attempt to make some general points with implications for DFT+*U* studies of O 2*p* holes in oxides.

Firstly we note that to describe consistently the electronic holes in the systems studied in the present work and in Li doped MgO (Ref. 7) show that a value of *U* of 7 eV is sufficient. This suggests that the description of the O 2*p* hole is independent of the oxide material. More importantly, there exists experimental data in which the on-site Coulomb interaction (*U*_{*p-p*}) for O 2*p* holes has been determined.^{22–24} Auger spectroscopy studies of different oxides demonstrate that the on-site Coulomb repulsion energy for a hole in an O 2*p* orbital is 5–7 eV, entirely consistent with the present work.^{22,23} A number of studies of specific systems also demonstrate that *U*_{*p-p*} is consistent with the value of *U* in the present work. These materials include SrCoO₃, for which *U*_{*p-p*} was determined to be 6 eV,²⁵ La₂CuO₄, for which *U*_{*p-p*} is 7.3 eV,²⁶ Sr₂CuO₃, for which *U*_{*p-p*} is 6 eV,²⁷ and for LaCoO₃ and LaFeO₃, for which *U*_{*p-p*} are 6.8 and 6.7 eV, respectively.²⁸ For transition metal oxides in general, Nekrasov *et al.*²⁹ used a value of 6 eV, close to the 5.9 eV determined from Auger spectroscopy.²³ These values are all consistent with each other and with value of *U* in the present work and Ref. 7.

Therefore, we can now suggest that for oxide materials in which an O 2*p* hole is present (which can generally be ascertained without recourse to experiment), DFT+*U* with a value of *U* of 7 eV for the O 2*p* states will be a suitable first principles approach, even where experimental data are lacking, providing a predictive capability for DFT+*U*. Of course,

this only holds for this specific class of materials. However, there are many oxide materials of great interest, e.g., copper-derived superconductors, in which O 2*p* holes are present, so that the implications of the present work are not merely confined to a narrow class of materials.

IV. CONCLUSIONS

The description of localized hole states in doped oxides is challenging for DFT. In agreement with previous studies, we have found that applying GGA to the question of the atomic and electronic structures of Al doped silica leads to an inconsistent description of the geometry around the defect as well as the electronic structure. Application of the DFT+*U* approach provides a consistent description of both the geometry and electronic structures. With *U*=7 eV, we find elongation of a single Al–O distance to 1.88 Å, in good agreement with experiment, while the remaining Al–O distances are significantly shorter. The density of states shows the presence of an unoccupied O 2*p* derived hole state, which lies 1.1 eV above the valence band, while a spin density analysis shows that the hole state is localized on the oxygen atom with the elongated Al–O distances. The energy of formation of the dopant is 5.7 eV. We have also discussed choosing *U* and the impact of different DFT+*U* implementations, as well as the case of no experimental data being available. We have demonstrated that for DFT+*U* calculations involving O 2*p* electronic holes, the value of *U* determined from fitting to experimental data for two different oxides is consistent with values of *U* determined from previous studies, using different experimental techniques. With the value of *U* for O 2*p* holes derived in the present work, a predictive capability for the DFT+*U* approach as a tool for studying O 2*p* holes in doped and defective oxide materials has been established.

ACKNOWLEDGMENTS

We acknowledge support for this work from the Donors of the Petroleum Research Fund administered by the American Chemical Society and Science Foundation Ireland (Grant No. 04/BR/C0216). We acknowledge the Trinity Centre for High Performance Computing for access to the TCHPC computational facilities through the IITAC project, funded by the HEA PRTL cycle 3.

¹V. I. Anisimov, J. Zaanen, and O. K. Andersen, Phys. Rev. B **44**, 943 (1991).

²M. Alfreðsson, G. D. Price, C. R. A. Catlow, S. C. Parker, R. Orlando, and J. P. Brodholt, Phys. Rev. B **70**, 165111 (2004).

³M. Nolan, S. C. Parker, and G. W. Watson, Surf. Sci. **595**, 226 (2005).

⁴S. Fabris, G. Vicario, G. Balducci, S. de Gironcoli, and S. Baroni, J. Phys. Chem. B **109**, 22860 (2005).

⁵A. B. Shick, W. E. Pickett, and A. L. Liechtenstein, J. Electron Spectrosc. Relat. Phenom. **114**, 753 (2001).

⁶H. T. Tohver, M. M. Abraham, Y. Chen, and B. Henderson, Phys. Rev. B **5**, 3276 (1972).

⁷M. Nolan and G. W. Watson, Surf. Sci. **586**, 25 (2005).

⁸R. H. D. Nuttall and J. A. Weil, Can. J. Phys. **59**, 1696 (1981).

⁹J. Laegsgaard and K. Stokbro, Phys. Rev. Lett. **86**, 2834 (2001).

¹⁰J. Laegsgaard and K. Stokbro, Phys. Rev. B **65**, 075208 (2002).

¹¹G. Pacchioni, F. Frigoli, D. Ricci, and J. A. Weil, Phys. Rev. B **63**, 054102 (2001).

¹²J. To, A. A. Sokol, S. A. French, N. Kaltsayannis, and C. R. A. Catlow,

- J. Chem. Phys. **122**, 144704 (2005).
- ¹³ S. L. Dudarev, G. A. Botton, S. Y. Savrasov, C. J. Humphreys, and A. P. Sutton, Phys. Rev. B **57**, 1505 (1998).
- ¹⁴ G. Kresse and J. Hafner, Phys. Rev. B **49**, 14251 (1994).
- ¹⁵ G. Kresse and J. Furthmüller, Comput. Mater. Sci. **6**, 15 (1996).
- ¹⁶ P. E. Blöchl, Phys. Rev. B **50**, 17953 (1994).
- ¹⁷ D. Joubert and G. Kresse, Phys. Rev. B **59**, 1758 (1999).
- ¹⁸ J. P. Perdew, K. Burke, and M. Eruzerhof, Phys. Rev. Lett. **77**, 3865 (1996).
- ¹⁹ V. I. Anisimov, I. V. Solovyev, M. A. Korotin, M. T. Czyzyk, and G. A. Sawatzky, Phys. Rev. B **48**, 16929 (1993).
- ²⁰ M. Gadjos and J. Hafner, Surf. Sci. **590**, 117 (2005).
- ²¹ M. Cococcioni and S. de Gironcoli, Phys. Rev. B **71**, 035105 (2005).
- ²² J. Ghijsen, L. H. Tjeng, J. van Elp, H. Eskes, J. Westerink, G. A. Sawatzky, and M. T. Czyzyk, Phys. Rev. B **38**, 11322 (1988).
- ²³ M. L. Knotek and P. J. Fiebelman, Phys. Rev. Lett. **40**, 964 (1978).
- ²⁴ I. S. Elfimov, S. Yunoki, and G. A. Sawatzky, Phys. Rev. Lett. **89**, 216403 (2002).
- ²⁵ R. H. Potze, G. A. Sawatzky, and M. Abbate, Phys. Rev. B **51**, 11501 (1995).
- ²⁶ A. K. McMahan, R. M. Martin, and S. Satpathy, Phys. Rev. B **38**, 6650 (1988).
- ²⁷ R. Neudert, S.-L. Drechsler, J. Malek *et al.*, Phys. Rev. B **62**, 10752 (2000).
- ²⁸ A. Chainani, M. Mathew, and D. D. Sarma, Phys. Rev. B **46**, 9976 (1992); **48**, 14818 (1993).
- ²⁹ I. A. Nekrasov, M. A. Korotin, and V. I. Anisimov, e-print cond-mat/0009107.